

## Influence on the Formation of Aragonite or Vaterite by Otolith Macromolecules

Giuseppe Falini,<sup>\*[a,b]</sup> Simona Fermani,<sup>[b]</sup> Silvia Vanzo,<sup>[c]</sup> Marin Miletic,<sup>[c]</sup> and Giulia Zaffino<sup>[b]</sup>

**Keywords:** Biomineralization / Otoliths / Vaterite / Aragonite / Calcium carbonate / Polymorphism / Bioinorganic chemistry

Calcium carbonate polymorphism is one of the most challenging problems in biomineralization. Calcium carbonate exists in three crystalline forms: calcite, aragonite and vaterite. Otoliths of teleost fishes are made of vaterite and aragonite, located in different sacs and never mixed together. This paper presents a biochemical characterization of the intracrystalline macromolecules associated to the vateritic and aragonitic phases of otoliths. Experimental evidences from cal-

cium carbonate overgrowth on the surface of otoliths and in vitro crystallization on the chitin-silk fibroin assembly organic matrix suggest that the intracrystalline macromolecules associated to the otolith influence the aragonite–vaterite polymorphism.

(© Wiley-VCH Verlag GmbH & Co. KGaA, 69451 Weinheim, Germany, 2005)

### Introduction

The term otolith refers to the ear bone of teleost fishes. These carbonatic structures are a part of the stato-acoustical organ of advanced fishes that corresponds to the inner ear (labyrinth) and is responsible for the ability to hear and the equilibrium sense. The labyrinth includes three connected semicircular canals and three otolithic organs consisting of the sacculus, utricle and lagena,<sup>[1–3]</sup> each of which contains an otolith called sagitta, asteriscus and lapillus respectively. The asteriscus and lapillus are usually millimetre sized, but the sagitta can range from millimetre to centimetre size.<sup>[1]</sup> As sagittae are the largest otolith, they have been widely utilized in teleost growth rate and age assessment studies.<sup>[1]</sup>

Crystals of otoliths, once deposited, are metabolically inert, except under extreme stress. Thus, the otolith can potentially retain the variation in crystalline structure due to variation in the organic matrix or in the crystallization environment.<sup>[1]</sup>

Biomineralization of otoliths differs from that of vertebrate bone, molluscan shell and coral skeleton since the otolith epithelium is not in direct contact with the region of calcification. As a result, the calcification is heavily dependent upon the composition of the endolymphatic fluid

surrounding the otolith.<sup>[4–6]</sup> However, the mineral crystalline units are associated with an organic matrix. Approximately half of the otolith matrix macromolecules are water insoluble<sup>[7]</sup> and, presumably, make up the structural framework for subsequent calcification. The soluble proteins are characterized by a high abundance of acidic amino acids, and are termed “otolin”.<sup>[8]</sup> The most recently elucidated otolith water-soluble protein is characterized by a high content of acidic amino acids and can control the calcium carbonate morphology and polymorphism.<sup>[9]</sup>

Different polymorphs of calcium carbonate are linked to the different otolith organs. While aragonite is normal in sagittae and lapillus, most asteriscus are made of vaterite.<sup>[10,11]</sup> Vaterite is also the principal polymorph in many abnormal otoliths.<sup>[12]</sup> There is no accepted explanation for the formation of vateritic otoliths together with aragonitic ones.<sup>[13]</sup> Vaterite precipitates in supersaturated solutions that are far from equilibrium,<sup>[14]</sup> alternatively, matrix proteins may mediate vaterite formation, similarly as described for calcite and aragonite in mollusc shells.<sup>[15]</sup>

We present here a characterization of the intracrystalline acidic macromolecules associated to aragonitic and vateritic otoliths. The influence of such macromolecules on calcium carbonate polymorphism in fish otoliths is also analyzed and discussed.

### Results

#### General Description

Figure 1 (a, b) gives a view of the otoliths lapillus and asteriscus of *Chondrostoma nasus nasus*. In the family of

<sup>[a]</sup> Environmental Chemistry Laboratory, University of Bologna, Via dell'Agricoltura 5, 48100 Ravenna, Italy  
<sup>[b]</sup> Department of Chemistry “G. Ciamician”, Alma Mater Studiorum University of Bologna, Via Selmi 2, 40126 Bologna, Italy  
Fax: (internat.) + 39-051-2099456  
E-mail: giuseppe.falini@unibo.it  
<sup>[c]</sup> Department of Biology, University of Trieste, Via Weiss 2, Trieste, Italy

Ciprinidi, sagitta is the smallest otolith, while lapillus and asteriscus can reach the size of millimetres. Their morphology has been well described.<sup>[13]</sup>

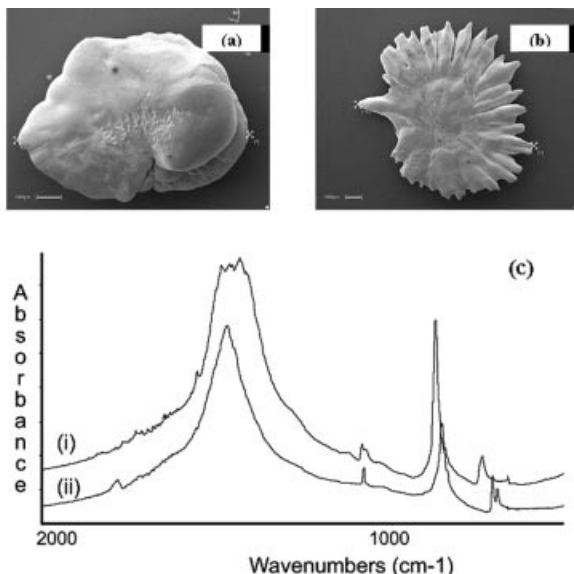


Figure 1. Scanning electron microscopy images of the anti-sulcal surface of otoliths lapillus (a) and asteriscus (b) from *Chondrostoma nasus nasus*; (c) FTIR spectra of asteriscus (i) and lapillus (ii) show the characteristic absorption peaks of vaterite and aragonite respectively<sup>[18]</sup>

Lapillus and asteriscus were used as sources of aragonitic and vateritic associated intracrystalline macromolecules, respectively (see c in Figure 1). The textural organization in lapillus and asteriscus (Figure 2) has locally radial oriented crystalline units that change in size as a function of the polymorph. Those of aragonite appear as a long prism with an average thickness of about 5  $\mu\text{m}$  (see a in Figure 2). Interestingly, this is the thickness of the crystalline units in the naere of the shells.<sup>[3]</sup> Vaterite crystalline units in the asteriscus appear as small needles locally oriented (see b in Figure 2). Each crystalline unit, of either aragonite or vaterite, is embedded completely in an organic matrix (Figure 2, c and d). This organic matrix is partially water insoluble and its structure is observable after decalcification in the presence of fixatives. It makes a continuous network that can bridge all the crystalline units (Figure 2, e and f). In the pictures the fixed organic matrix appears to be full of holes and small fragments; we cannot exclude that this is an artifact of the drying process, as has been shown for others organic matrices.<sup>[16]</sup>

#### Acidic Macromolecules Associated to Aragonite and Vaterite

Cation exchange resin was used to extract the acidic intracrystalline macromolecules from the otoliths.<sup>[17]</sup> SDS-PAGE, amino acid analysis and FTIR spectroscopy were used to characterize the soluble macromolecules extracted from lapillus and asteriscus.

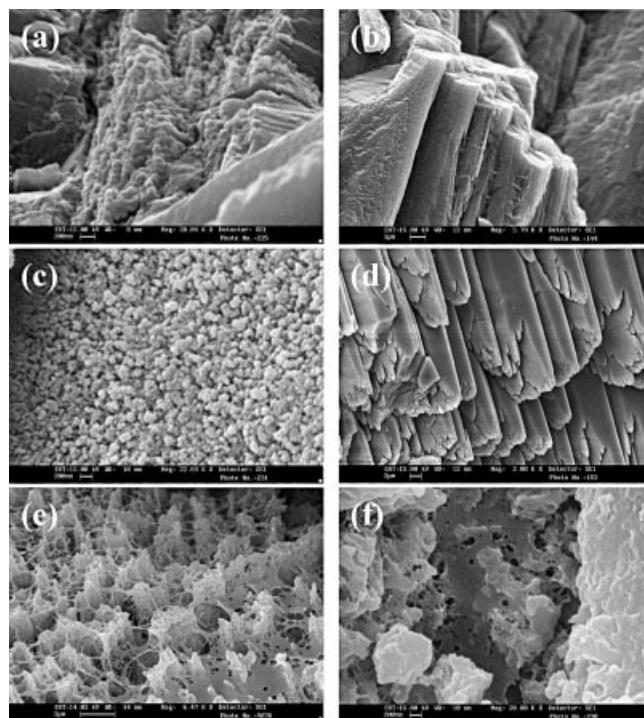


Figure 2. Scanning electron microscopy images of the textural organization of crystalline units in asteriscus (a) and (c) and lapillus (b) and (d); in (e) and (f) the insoluble organic matrix after fixation associated to asteriscus and lapillus respectively is shown

Figure 3 compares the major otoliths proteins of the two calcium carbonate polymorphs, aragonite and vaterite. In lines numbered 1 the molecular weight markers are reported, while lines 2–4 show the running gels of the soluble macromolecular assembly extracted from asteriscus (2), and lapillus (3, 4) at different concentrations. In the macromolecular gel lines some material was retained close to the top and a main band at about 67000 was observed. Other weak bands at higher molecular weight are present. However, there are differences between the macromolecules associated to aragonite (lines 3 and 4) and those associated to vaterite (line 2). Those associated to aragonite show a second main band at about 30000 while those of vaterite show a strong at about 40000. Many other minor bands are present in both the aragonitic- and vateritic-soluble macromolecular assemblies. Table 1 gives the amino acid composition of the proteic part of the soluble macromolecular assembly associated with aragonite (lapillus) and vaterite (asteriscus) in the otoliths. The total amino acid composition is quite similar; the main difference is a higher content of Glx in the macromolecules associated to vaterite. Figure 4 reports the FTIR spectra of intracrystalline soluble macromolecules associated to lapillus (aragonitic) and asteriscus (vateritic).

A protein amide I absorption band at 1654  $\text{cm}^{-1}$  and a large absorption band at around 1100  $\text{cm}^{-1}$  dominate the infrared spectrum of the ensemble of macromolecules from asteriscus (Figure 4).<sup>[18]</sup>

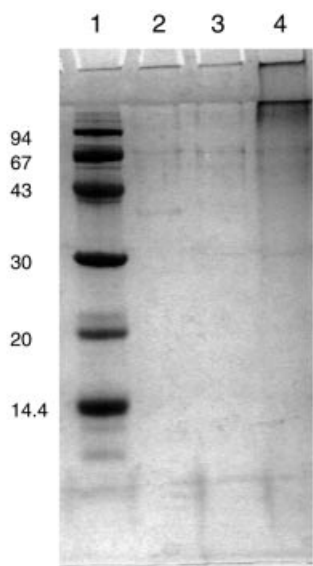


Figure 3. SDS-PAGE of acidic macromolecules extracted from *Chondrostoma nasus nasus* aragonitic (line 3, 4) or vateritic (50 ng, line 2) otoliths; concentrations of aragonitic acidic macromolecules of 10 and 50 ng were used in lines 3 and 4 respectively; in line 1, hmw markers are reported

Table 1. Amino acid composition of the proteic parts associated with the soluble macromolecules extracted from the otoliths asteriscus and lapillus; the last row gives the proteic concentration in the mineral phase

	Otoliths	
	Asteriscus	Lapillus
Asx	19.34	19.24
Thr	7.84	8.50
Ser	12.92	11.69
Glx	14.29	10.06
Pro	6.13	5.55
Gly	9.18	10.06
Ala	8.82	7.85
Cys	0.19	0.00
Val	4.95	4.84
Met	1.34	1.30
Ile	1.72	2.11
Leu	3.77	3.99
Tyr	0.80	1.13
Phe	1.73	1.87
Lys	4.04	4.56
His	1.87	2.65
Arg	1.08	1.25
ppm	427	474

The IR spectrum of the lapillus macromolecules shows bands at 1100 and 1255  $\text{cm}^{-1}$ , protein amide I absorption at 1653  $\text{cm}^{-1}$ , and relatively strong carboxylate absorption bands at around 1575 and 1417  $\text{cm}^{-1}$ .

### In vitro Crystal Growth

SEM images of the mineral phases obtained from the overgrowth experiments are shown in Figure 5. Large

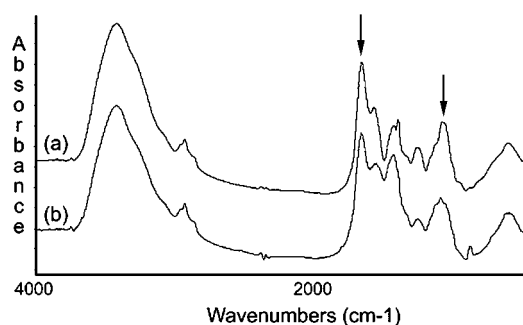


Figure 4. FTIR spectra of ground samples (tens of micrograms) in KBr pellets of acidic macromolecules extracted from *Chondrostoma nasus nasus* vateritic (a) or aragonitic (b) otoliths; arrows indicate the main absorption bands associated with the proteic and glycosidic regions of the acidic macromolecules

rhombohedral crystals, along with many small needle-like ones, form on the surface of lapillus (Figure 5, b). The latter crystals almost completely cover the surface, with a few big rhombohedral crystals grown among them (Figure 5, d). Comparison with known morphologies of calcium carbonate polymorphs indicates that the rhombohedral ones are calcite while the needle-like ones are aragonite<sup>[3]</sup> (Figure 5, e).

On the asteriscus surface, however, the overgrowth of calcium carbonate produced different results. The calcite crystals are no longer well separated and grow in clusters on small regions of the asteriscus surface (Figure 5, a). Together with the typical {104} rhombohedral faces, the crystals show specific additional faces (Figure 5, c) that are more pronounced in the centre of the otoliths than on the edge. These additional faces are almost parallel to the calcite *c* axis. In some surface regions, aggregates of plate-like crystals were seen (Figure 5, e) that show a similar morphology to that of synthetic vaterite.<sup>[3]</sup>

Crystallization experiments of calcium carbonate were also carried out on a silk-fibroin/ $\beta$  chitin assembly in which the soluble macromolecules extracted from lapillus and asteriscus were adsorbed (Table 2). In all crystallization experiments, a mixture of calcite and vaterite was obtained. Calcite was observed on the substrate surface as small single crystals, with a rhombohedral appearance, while vaterite crystallized as crystalline aggregated spherulites (Figure 6, a and b). The mineral phase was identified by an FTIR technique (Figure 6, c).<sup>[18]</sup>

In the controls system, where no acidic macromolecules were adsorbed, calcite, as the main phase, and vaterite were formed. The pH at the end of the crystallization experiment was 7.8 and the average number of crystals (calcite plus vaterite) was about 9.6 per  $\text{cm}^2$ . In the presence of adsorbed acidic macromolecules extracted from lapillus, both calcite and vaterite were observed. However, with respect to the control, a higher density of crystallization was observed (about 26.6 crystal per  $\text{cm}^2$ ), even if the average size, the polymorphic distribution and the final pH of the crystallization media were almost the same. A different scenario

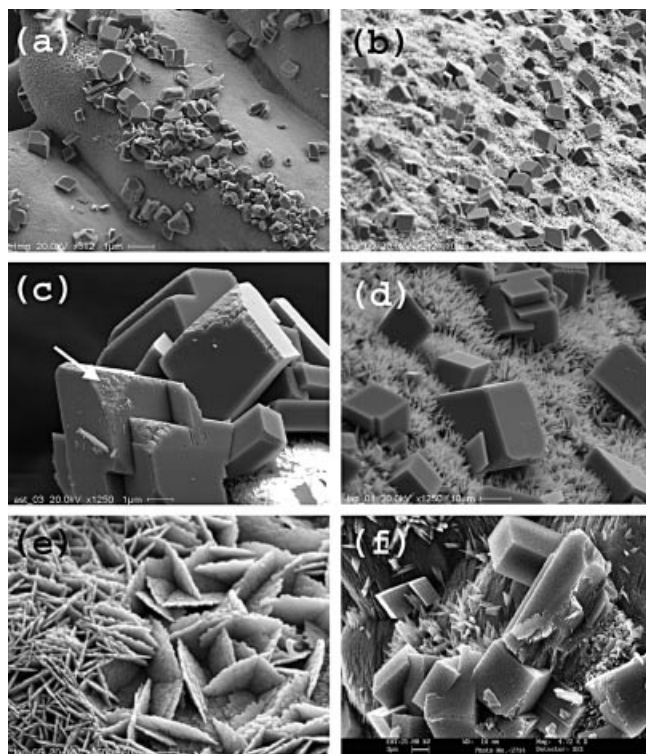


Figure 5. Scanning electron microscopy images of calcium carbonate crystal overgrown on the surface of otoliths asteriscus (a, c, e) and lapillus (b, d, f). (a) and (b); general overview of the calcium carbonate overgrown on the otoliths surface; (c) and (d) show calcite crystals; note the different morphology; calcite crystal overgrown on the asteriscus surface shows an additional face (marked by an arrow and indexed  $\{hk0\}$ ) with respect to those overgrown on lapillus surface, which show only the typical  $\{104\}$  rhombohedral faces; (e) vaterite plate-like crystals overgrown on asteriscus surfaces; (f) aragonite needle-like crystals overgrown on the lapillus surface

Table 2. Calcium carbonate polymorphs obtained on the silk fibroin  $\beta$ -chitin assembly in the presence of soluble acidic macromolecules extracted from aragonitic (lapillus) or vateritic (asteriscus) otoliths

Mineral phase <sup>[b]</sup>	Control <sup>[a]</sup>	Lapillus	Asteriscus
	C + V	C + V	C + V
Longest crystal axis <sup>[c]</sup> [mm]	0.05 0.08	0.05 0.08	0.05 0.23
Crystals density <sup>[d]</sup> [ $m/cm^2$ ]	9.6	26.6	26.6
Final pH <sup>[e]</sup>	7.8	7.8	8.2

<sup>[a]</sup> No additives added to the silk fibroin  $\beta$ -chitin assembly in the control experiment. <sup>[b]</sup> Main calcium carbonate polymorph in bold. <sup>[c]</sup> Average longest axis of the calcite crystals (first row) and average diameter of the spherulite of vaterite (second row). <sup>[d]</sup> Crystal density measured by counting crystalline units under an optical microscope. <sup>[e]</sup> Final pH of the aqueous media in which the crystallization process took place.

occurred in the presence of acidic macromolecules extracted from asteriscus. The spherulites of vaterite appeared bigger than those formed on the control, and the final pH of the crystallization media increased with respect to the control, from 7.8 to 8.2.

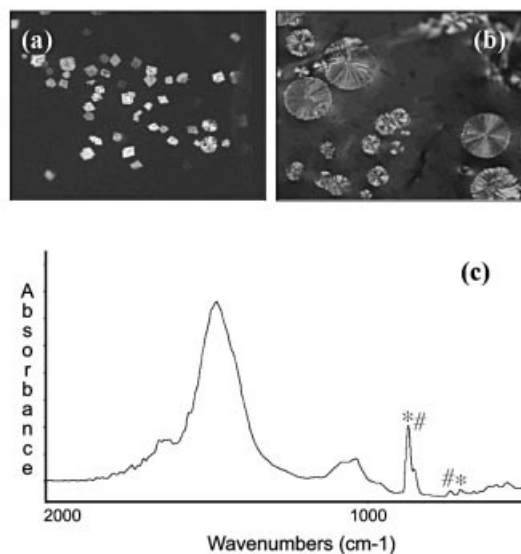


Figure 6. Optical micrographs in cross polar of calcium carbonate aggregates grown in the  $\beta$ -chitin/silk fibroin assembly with or without acidic macromolecules extracted from *Chondrostoma nasus* aragonitic or vateritic otoliths; (a) calcite crystals and a few vaterite spherulites formed in the presence of aragonite associated acidic macromolecules; (b) vaterite spherulites and a few calcite crystals formed in the presence of vaterite associated acidic macromolecules; magnification 40 $\times$ ; (c) FTIR spectrum of the mineral phases associated to the  $\beta$ -chitin/silk fibroin assembly, showing absorption peaks characteristic of vaterite (\*) and calcite (#)<sup>[18]</sup>

## Discussion

Otoliths of the teleost fish *Chondrostoma nasus nasus* are deposits of calcium carbonate formed of aragonite and vaterite. Intracrystalline acid macromolecules associated at these two mineral phases have been studied. They are an assembly of proteins and glycoproteins with a wide range of molecular weights. A main band at about 67 000 seems to be common to both mineralized tissues. Differences are present in minor bands. A band at about 30 000 seems to be characteristic of lapillus macromolecules while one at about 40 000 is observed only in asteriscus macromolecules. This latter band has been reported previously.<sup>[19]</sup> The amino acid composition shows no strong, significant differences between the proteic regions of the acidic macromolecules extracted from aragonitic and vateritic otoliths. However, vateritic ones have a higher Glx content. High Glx contents have also been observed in acidic macromolecules associated to amorphous calcium carbonate.<sup>[20]</sup> If we consider that amorphous calcium carbonate has the highest solubility among calcium carbonates, and that vaterite is the most soluble calcium carbonate crystalline phase, we could speculate that a high Glx content may be associated with highly soluble calcium carbonate mineral phases.

FTIR spectra of the two families of acidic macromolecules show different absorptions in the region typical of carbohydrates (around 1000  $cm^{-1}$ ), suggesting a different degree of glycosilation. These differences may be correlated with the SDS-PAGE bands.

The control of acidic macromolecules over the mineral deposition was tested using two crystallization systems. Overgrowth experiments are a powerful tool to evaluate the effect of acidic macromolecules on mineral deposition since they are in a conformation that in many aspects is the closest to the native one. Two different families of mineral grew on the surface of the aragonitic lapillus. Calcite crystals grew with a regular rhombohedral habit, suggesting that no macromolecules interacted with them. These crystals do not show a preferential direction of growth, although this is not easy to state since the lapillus surface is quite rough. Together with the calcite crystals, many much smaller plate-like crystals of aragonite were observed (ca. 1  $\mu\text{m}$  versus more than 20  $\mu\text{m}$  for calcite). These crystals almost completely covered the surface and gathered in clusters with no preferential orientation.

A different scenario appears on the asteriscus surface after the overgrowth experiments. The calcite crystals show a new crystalline face with respect to the regular rhombohedral calcite. This new face, almost parallel to the calcite *c* axis, has been observed previously by Albeck et al.<sup>[21]</sup> It was associated to a specific interaction of one (or more) soluble macromolecule(s) on a specific crystalline plane, stabilizing it and producing its appearance. This new face on the calcite crystals is more evident in the central part of the asteriscus than on the edges. This may be explained in terms of a higher concentration of the released macromolecules in the surrounding media of those regions.

On the surface of asteriscus, in regions distant from the calcitic one, vaterite was also observed. This polymorphic spatial specification could be associated to a different etching and hence to a different release of acidic macromolecules.

These observations indirectly confirm the SDS-PAGE and FTIR observations. The two families of acidic macromolecules associated to the aragonitic and vateritic otoliths are composed of different macromolecules, and they can interact with growing calcium carbonate in different ways.

Aragonite forms on the surface of aragonitic biomaterial<sup>[22]</sup> but, to our knowledge, this is the first example of the overgrowth of vaterite on a vateritic biomineral, under conditions where calcite precipitation is favored.

The ability of the acidic macromolecules to influence calcium carbonate polymorphism has also been tested using an artificial assembly made of silk fibroin and  $\beta$ -chitin. The silk-fibroin/ $\beta$  chitin assembly is not strictly relevant in otolith biomineralization, since neither  $\beta$ -chitin nor silk fibroin-like proteins has been shown to be present in the otolith insoluble matrix. However, this artificial assembly has been used successfully to verify the nucleating properties of acidic macromolecules extracted from mollusc shells. In search of an analogy between these two mineralized tissues, we used it to run crystallization experiments. Calcite and vaterite were observed in all crystallization experiments, irrespective of the presence of the acidic macromolecules. However, some interesting features arise from the crystallization results (Table 2). The substrate in which acidic macromolecules extracted from the lapillus were adsorbed

showed no differences to the control in terms of polymorph distribution, crystal size and final chemical properties of the surrounding media. Calcite was the main crystalline phase, with few vaterite spherulites. The density of crystallization on the surface increased, suggesting that these charged macromolecules, once adsorbed on a substrate, favor the nucleation and growth of calcium carbonate.<sup>[23]</sup> No evidence for aragonite was obtained. This indicates that the artificial assembly does not cover the requirement for the acidic macromolecules' polymorphic control, or that these proteins are unable to control aragonite formation. In this case, a pure physical control should be addressed. In the presence of the acidic macromolecules extracted from the asteriscus the final pH of the crystallization media increased with respect to those of the control and lapillus (Table 2) and larger spherulites of vaterite made up the main phase on the matrix surface. This means that the system reached equilibrium at a higher supersaturation than did the control, justifying the formation of vaterite in the matrix.<sup>[24]</sup> Vaterite is metastable in water solution and spontaneously transforms into calcite;<sup>[25]</sup> the presence of large vaterite spherulites suggests that the system acidic macromolecules from asteriscus—artificial assembly favors and stabilizes vaterite formation.

## Conclusion

Intracrystalline acidic macromolecules of otoliths influence calcium carbonate polymorphism. A preliminary characterization of these acidic macromolecules has been carried out, and their calcium carbonate nucleating properties have been tested using overgrowth and substrate-mediated approaches.

## Experimental Section

**Materials:** Otoliths for this study were taken from the head of the fish *Chondrostoma nasus nasus* collected from the Isonzo river (Italy). After dissecting them from the fish ears, they were washed with sodium hypochlorite for 1 h to remove any organic superficial contaminant, then with Milli-Q water, and finally air-dried. No distinction was made between sex and left or right ear otoliths.

**Morphological Investigations:** Scanning electron microscopy (SEM) images were obtained by means of a Philips XL20 electron microscope on samples glued on an aluminium stub and gold sputtered. Prior to observations some otolith samples were mechanically broken to observe the inner morphology or decalcified in the presence of fixative to observe the insoluble organic matrix.<sup>[11]</sup>

**Protein Extraction:** Proteins were extracted using the cation exchange resin procedure.<sup>[24]</sup> Specifically, ground otoliths powder was poured into dialysis tubes and suspended in water (20 mL per 1.5 g of otolith). The sealed dialysis tube was then placed in a plastic cylinder. About one quarter of the cylinder, outside the dialysis tube, was filled with prewashed cation exchange resin and water was added to fill the cylinder. The cylinder was then closed with a stopper and rotated slowly and continuously in a propeller-like mode at room temperature to keep the powder and the resin in

suspension. The water outside the dialysis tube was changed twice per day. Decalcification was complete in about three days, and the absence of mineral was checked by IR spectroscopy. The content of the dialysis tube was then dialyzed against water for two days. The resulting soluble and insoluble material inside the dialysis tube was subsequently separated by centrifugation. The final soluble material was then concentrated by lyophilization.

**Polyacrylamide Gel Electrophoresis of Proteins:** Tris-tricine ready-to-use Minigels of 15% polyacrylamide were employed. The gel ran at 100 V for 1.5–2 h and was developed with Blue Coomassie.

**FTIR Spectrometry:** IR analyses were carried out on dried soluble and insoluble matrices. Calcium carbonate formed in the chitin–silk fibroin assembly was removed mechanically before analysis. All spectra were recorded at 4 cm<sup>-1</sup> resolution with a 32 scan with a Perkin-Elmer Model 1600 Fourier Transform Infrared Spectrometer (FTIR) from 4000 to 450 cm<sup>-1</sup>. Powder sample and KBr were dried under a red lamp, carefully mixed in a mortar, and pelleted with a press. A background spectrum was measured for pure KBr.

**In vitro Crystal Growth:** Two types of crystallization experiments were performed. Calcium carbonate crystals were overgrown on cleaned otoliths, or crystals were grown *de novo* in the presence of the soluble total macromolecular assemblage extracted from lapillus or asteriscus adsorbed on β-chitin and silk fibroin substrate.<sup>[15]</sup> The crystal growth procedure has been detailed previously.<sup>[26,27]</sup> Briefly, synthetic calcium carbonate crystals were grown for four days in a closed box, by slow diffusion of ammonium carbonate vapor into plastic Petri dishes containing the otoliths, or the nucleating substrate, overlaid by a 10 mM CaCl<sub>2</sub> solution. The obtained calcium carbonate crystals were rinsed with Milli-Q water, observed under optical microscope, and successively air-dried. For detailed morphological analysis, the crystals were gold coated and observed by SEM

## Acknowledgments

This work was supported by MIUR (Cofin 2003), CNR and the University of Bologna (Funds for Selected Research Topics).

<sup>[1]</sup> S. E. Campana, *Mar. Ecol.: Prog. Ser.* **1999**, *188*, 263–297.

<sup>[2]</sup> O. Lowenstain, *Br. Med. Bull.* **1956**, *12*, 110–4.

<sup>[3]</sup> H. A. Lowenstain, S. Weiner, *On Biomineralization*, Oxford University, Press New York, **1989**.

- <sup>[4]</sup> P. Payan, H. Kossmann, A. Watrin, N. Mayer-Gostan, G. Boeuf, *J. Exp. Biol.* **1997**, *200*, 1905–1912.
- <sup>[5]</sup> P. Payan, G. Borelli, G. Boeuf, N. Mayer-Gostan, *Fish Physiol. Biochem.* **1998**, *19*, 35–41.
- <sup>[6]</sup> L. Addadi, S. Weiner, *Angew. Chem.* **1992**, *31*, 153–169; *Angew. Chem. Int. Ed. Engl.* **1992**, *31*, 153–169.
- <sup>[7]</sup> M. Asano, Y. Mugiya, *Comp. Biochem. Physiol., Part B: Biochem. Mol. Biol.* **1993**, *104*, 201–205.
- <sup>[8]</sup> T. E. Degens, W. G. Deuser, R. L. Haedrich, *Mar. Biol.* **1969**, *2*, 105–13.
- <sup>[9]</sup> C. Soellner, M. Burghammer, E. Busch-Nentwich, J. Berger, H. Schwarz, C. Riekel, T. Nicolson, *Science* **2003**, *302*, 282–286.
- <sup>[10]</sup> A. M. Oliveira, M. Farina, I. P. Ludka, B. Kachar, *Naturwissenschaften* **1996**, *83*, 133–135.
- <sup>[11]</sup> D. Lenaz, M. Miletic, *Neues Jahrb. Mineral., Monatsh.* **2000**, *11*, 522–528.
- <sup>[12]</sup> R. W. Gaultie, S. K. Sharma, E. Volk, *Comp. Biochem. Physiol., Part A: Mol. Integr. Physiol.* **1997**, *118*, 167–194.
- <sup>[13]</sup> R. W. Gaultie, *J. Morphol.* **1993**, *218*, 1–28.
- <sup>[14]</sup> D. Kralj, L. Brecevic, A. E. Nielsen, *J. Cryst. Growth* **1990**, *104*, 793–800.
- <sup>[15]</sup> G. Falini, S. Albeck, S. Weiner, L. Addadi, *Science* **1996**, *271*, 67–9.
- <sup>[16]</sup> Y. Levi-Kalishman, G. Falini, L. Addadi, S. Weiner, *J. Struct. Biol.* **2001**, *135*, 8–17.
- <sup>[17]</sup> D. Worms, S. Weiner, *J. Exp. Zool.* **1986**, *237*, 11–20.
- <sup>[18]</sup> W. B. White in *Infrared Spectra of Minerals* (Ed.: V. C. Farmer), Mineralogical Society, London, **1974**, pp. 227–284.
- <sup>[19]</sup> B. A. Gotliv, L. Addadi, S. Weiner, *ChemBioChem.* **2003**, *4*, 522–529.
- <sup>[20]</sup> J. Aizenberg, G. Lambert, L. Addadi, S. Weiner, *Adv. Mater.* **1996**, *8*, 222–6.
- <sup>[21]</sup> S. Albeck, S. Weiner, L. Addadi, *Chem. Eur. J.* **1996**, *2*, 278–84.
- <sup>[22]</sup> S. Blank, M. Arnoldi, S. Khoshnavaz, L. Treccani, M. Kuntz, K. Mann, G. Grathwohl, M. Fritz, *J. Microsc. (Oxford, U.K.)* **2003**, *212*, 280–291.
- <sup>[23]</sup> L. Addadi, S. Weiner, *Proc. Natl. Acad. Sci. U. S. A.* **1985**, *82*, 4110–14.
- <sup>[24]</sup> G. Falini, S. Fermani, M. Gazzano, A. Ripamonti, *Chem. Eur. J.* **1998**, *4*, 1048–1052.
- <sup>[25]</sup> D. Kralj, L. Brecevic, J. Kontrec, *J. Cryst. Growth* **1997**, *177*, 248–257.
- <sup>[26]</sup> S. Albeck, L. Addadi, S. Weiner, *Connect. Tissue Res.* **1996**, *35*, 365–370.
- <sup>[27]</sup> J. Aizenberg, S. Albeck, S. Weiner, L. Addadi, *J. Cryst. Growth* **1994**, *142*, 156–64.

Received May 20, 2004

Early View Article

Published Online November 18, 2004